Polymer Degradation and Stability 167 (2019) 179–188

Contents lists available at ScienceDirect

Polymer Degradation and Stability

journal homepage: www.elsevier.com/locate/polydegstab

Synthesis of an effective bio-based flame-retardant curing agent and its application in epoxy resin: Curing behavior, thermal stability and flame retardancy

Zong-Min Zhu [a, *], Ke Shang [b], Luo-Xin Wang [a], Jun-Sheng Wang [b, **]

[a] College of Materials Science and Engineering, State Key Laboratory of New Textile Materials and Advanced Processing Technologies, Wuhan Textile University, Wuhan, 430200, Hubei, PR China
[b] Tianjin Fire Research Institute of the Ministry of Public Security, Tianjin, 300381, PR China

ARTICLE INFO

Article history:
Received 26 May 2019
Received in revised form
1 July 2019
Accepted 7 July 2019
Available online 8 July 2019

Keywords:
Epoxy resin
Bio-based curing agent
Flame retardancy
Smoke suppression
Thermal behavior
Mechanism

ABSTRACT

In this work, a bio-based macromolecule ammonium phytic acid named as PA-AEP was synthesized successfully via neutralization reaction between phytic acid (PA) and N-aminoethylpiperazine (AEP) and served as a monocomponent flame-retardant curing agent to improve the flame retardancy and smoke suppression of epoxy resin (EP). Curing behavior, flame retardancy and combustion behavior of PA-AEP cured epoxy resin were investigated. By comparison with EP/AEP reference sample, EP/PA-AEP samples showed good flame retardancy and smoke suppression effect because of the addition of PA-AEP. The PA-AEP cured EP sample passed UL-94 V-0 rating and achieved to a limiting oxygen index (LOI) value of 28.0% with 20 wt% PA-AEP. Cone calorimeter test results showed that, compared with EP/20% AEP reference sample, both the peak of heat release rate (PHRR), total heat release (THR), the peak of smoke production release (SPR) and total smoke production (TSP) of EP/20 wt% PA-AEP sample were decreased by 44.4%, 55%, 49% and 80.8%, respectively. In addition, by analyzing the char residues and volatile pyrolysis products, it was concluded that PA-AEP mainly played an important role in condensed phase which was associated with the formation of phosphorus-rich intumescent char layer.

1. Introduction

Epoxy resin (EP) has been widely used in the fields of electronic appliances, aerospace and coatings because of its good cohesiveness, chemical and corrosion resistance and outstanding mechanical properties etc [1–3]. However, the drawbacks of high flammability and lots of smoke during combustion restrict its application in many areas to a certain degree.

In this regard, several approaches have been proposed to solve these defects. Adding halogenated flame retardants (HFRs) is the most economical and effective method to achieve expected flame retardancy due to its low cost and high efficiency [4,5]. Unfortunately, many HFRs produce numerous toxic products and smoke during burning, which are harmful to the ecological environment and human health. Recent decades, halogen-free flame retardants (HFFRs), particularly phosphorus-containing flame retardants have attracted extensive attention thanks to high flame-retardant efficiency [6–8]. Phosphorus element or phosphorus-containing groups can be introduced into epoxy resins matrix by physically blending or chemically bonding. Comparatively, chemical bonding, also known as reactive flame-retardant method including reactive flame-retardant monomer [9–13] and reactive flame-retardant curing agent [14–19], can endow EP more durable flame retardancy. Among these phosphorus-containing groups, 9,10-dihydro-9-oxa-10-phosphaphenanthrene-10-oxide (DOPO) is often used in preparation of flame-retardant EP. By introducing DOPO groups into the polymer network can greatly enhance the flame retardancy of EP, but it has to compromise on lots of smoke production of EP. For instance, Xu et al. [20]. synthesized a novel phosphorus-containing imidazole-based curing agent (IHODOPO) from DOPO and imidazole for EP. The cured EP sample containing 15 wt% IHODOPO achieved UL-94 V-0 rating and produced less heat release. However, the total smoke production was not suppressed instead of increased. Intumescent flame-retardant (IFR) is

* Corresponding author.
** Corresponding author.
E-mail addresses: zhuzmgiant@126.com (Z.-M. Zhu), wangjunsheng@tfri.com.cn (J.-S. Wang).

https://doi.org/10.1016/j.polymdegradstab.2019.07.005
0141-3910/

considered to be a promising method for imparting EP with expected flame retardancy, more importantly, which can effectively achieve smoke suppression effect due to its condense phase flame-retardant activity [21]. Typical IFR system consists of an acid source, a carbon source and a gas source. Once the materials containing IFR are ignited, expanded carbon layer will be formed by esterification, carbonization and expansion processes, which can insulate the transfer of oxygen and heat simultaneously plays a role on smoke suppression and fire resistance. In our previous works [22], we prepared a novel IFR-EP system based on ammonium polyphosphate (APP) and a novel charring agent, which presented good flame retardancy and much lower production of smoke.

Besides, considering the environmental protection and the usage of renewable flame retardant resources, bio-based flame retardants like chitosan (CS) [23–26], phytic acid (PA) [27–30] and alginate [31] are used to construct flame-retardant system in recent years. Among them, phytic acid mainly comes from seed and root of plant and possess relatively high phosphorus content of 28 wt%, which can provide both acid and carbon source for intumescent flame retardants. Wang et al. [32]. prepared an additive type phytic acid salt intumescent flame retardant based on PA and melamine, and it gave EP with good flame retardancy and smoke suppression effect.

Hence, in order to solve the flammability and lots of smoke production defects simultaneously endow EP more durable flame retardancy, a bio-based macromolecule ammonium phytic acid was designed and prepared to construct reactive intumescent flame-retardant EP. In this paper, through simple neutralization reaction between PA and N-aminoethylpiperazine (AEP), the macromolecule ammonium phytic acid named PA-AEP was successfully prepared. The secondary amines in PA-AEP molecule acted as reactive sites with epoxy groups, while phytic acid groups endowed EP with good flame retardacy, making it a flame-retardant curing agent. Therefore, a series of PA-AEP cured flame-retardant EP materials were prepared and studied. The results of LOI, UL-94, and cone calorimeter tests proved that the PA-AEP was an effective flame-retardant curing agent for EP. The smoke suppression and flame retardancy of the PA-AEP cured EP samples were promoted significantly. Meanwhile, the flame-retardant mechanism was also discussed. The results of this paper will provide a theoretical basis for the development of bio-based flame-retardant curing agents with similar structures.

2. Experimental

2.1. Materials

Diglycidyl ether of bisphenol A (DGEBA, E−44) was obtained by Nantong Xingchen Synthetic Material Co., Ltd. (Nantong, China). Phytic acid aqueous solution (70%) and N-aminoethylpiperazine (99%) was purchased by Aladdin Chemistry Co., Ltd. (China). Anhydrous ethanol (99%) was from by Sinopharm Chemical Reagent Co., Ltd. (Shanghai, China). Distilled water was provided by our Lab.

2.2. Synthesis of macromolecule ammonium phytic acid (PA-AEP)

At room temperature, first, 18.86 g of 70% phytic acid aqueous solution (0.02 mol) was dissolved in 150 ml of distilled water. Then, 15.5 g of N-aminoethylpiperazine (0.12 mol) was added into the above aqueous solution, and the mixture kept stirring for 20 min. Subsequently, the crude product was obtained by removing the water with rotary evaporation and was washed ethanol several times. Finally, the blackish green powder was dried in vacuum oven at 60 °C for 8 h.

2.3. Preparation of the cured epoxy resins

The EP/AEP was obtained by traditional thermal curing process as reference. The air bubbles in DGEBA were removed under vacuum, and then AEP was added into DGEBA with continuous stirring. Once the mixture became a homogeneous solution, it was rapidly poured into prepared PTFE mold. Subsequently, the mixture was cured at 150 °C for 4 h. The flame-retardant EP was prepared in a similar process with a little difference. First, the PA-AEP (curing agent) and DGEBA were mixed together and stirred at 120 °C under vacuum condition until no bubbles appeared. Afterwards, the blends were transferred to PTFE mold. The higher the addition content of curing agent PA-AEP meant the faster the curing rate. EP/15% PA-AEP, EP/20% PA-AE and EP/25% PA-AEP were obtained after curing at 200 °C for 15, 12 and 10 h. Formulation of epoxy samples were shown in Table 1. EP/x% PA-AEP, where x wt% represented the weight percentage of PA-AEP in epoxy resins.

2.4. Characterization

Fourier transform infrared spectra (FT-IR) (400-4000 cm^{-1}) of samples were recorded (KBr pellets) at rt from a Nicolet 6700 FTIR instrument.

^1H nuclear magnetic resonance (NMR) spectra of samples were collected with a Bruker Ascend 400 spectrometer using D_2O as the solvent.

X-ray photoelectron spectroscopy (XPS) spectra of samples were recorded using a K-Alpha+ (Thermo fisher Scientific Co., USA) with Al Ka excitation radiation (hv = 1486.6 eV) under ultrahigh vacuum condition.

Thermogravimetry analysis (TG) was obtained on thermogravimetric analyzer (TGA4000, USA). The samples (about 7 mg) were heated from 40 °C to 800 °C at a heating rate of 10 °C/min under nitrogen. The volatile pyrolysis products decomposed from TG were connected by coupling FT-IR.

Glass transition temperature (T_g) of EP/AEP and EP/PA-AEP samples was measured by a PE instrument 4000 differential scanning calorimeter (DSC) from 30 °C to 150 °C at a heating rate of 10 °C/min under N_2 atmosphere. The non-isothermal curing kinetics of DGEBA/PA-AEP samples were carried on a DSC 4000 instrument (PE, USA) from 30 °C to 250 °C at different heating rates (5, 10, 15 and 20 K/min) under N_2 atmosphere.

Limiting oxygen index (LOI) values were tested by a HC-2C

Table 1
Formulation of EP/AEP and EP/PA-AEP samples and its LOI and UL-94 test results.

Sample	DGEBA(wt%)	AEP(wt%)	PA-AEP(wt%)	LOI(%)	UL-94 (3.2 mm)			
					av-t_1[a](s)	av-t_2[a](s)	Rating	Dripping
EP/20% AEP	80	20	0	21.5 ± 0.2	>60	–	NR	Yes
EP/15% PA-AEP	85	0	15	26.0 ± 0.5	47	1.5	NR	No
EP/20% PA-AEP	80	0	20	28.0 ± 0.5	3.5	2	V-0	No
EP/25% PA-AEP	75	0	25	32.4 ± 0.5	2	0.5	V-0	No

[a] Average combustion duration after the first (t_1) and the second ignition (t_2).

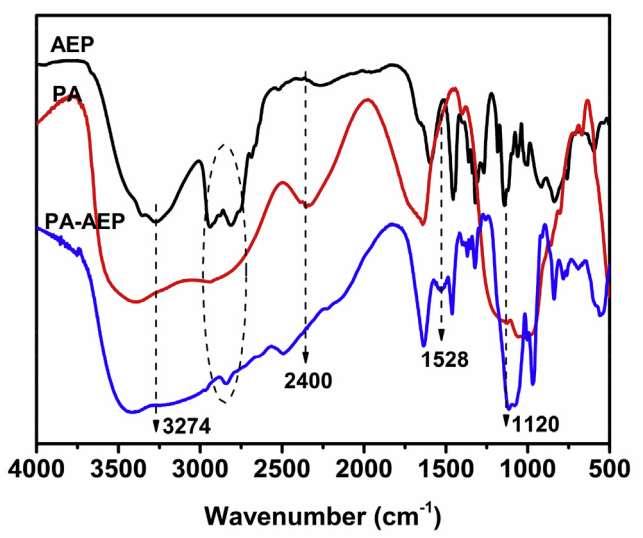

Fig. 1. IR spectra of AEP, PA and PA-AEP.

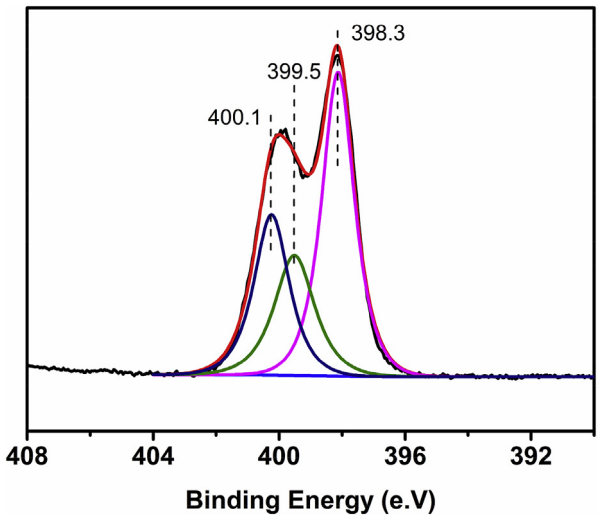

Fig. 3. N_{1s} XPS spectra of PA-AEP.

oxygen index meter (Jiangning, China) with sheet sizes of 130 × 6.5 × 3.2 mm according to ASTM D2863-97. The LOI tests for each spline were repeated three times, the results were the average of the three parallel tests. UL-94 rating level was measured on a CZF-4 instrument (Jiangning, China) and the size of sheets was 130 × 13 × 3.2 mm according to ASTM D3801. The fire behavior of samples was investigated using a cone calorimeter (Fire Testing Technology, UK) according to ISO5660-1. Each sample with size of 100 × 100 × 3.2 mm was exposed to a radiant cone at a heat flux of 35 kW/m^2. The data were obtained from the two parallel tests.

The carbon structure of cured EP samples after cone calorimeter test was analyzed by a LabRAM HR800 laser Raman spectrometer (SPEX Co.) with a 532 nm helium-neon laser line at room temperature.

The morphologies of char residues for cured EP samples after cone calorimeter test were observed by a JEOL JSM-5900LV scanning electron microscopy (SEM) instrument. The char layers were tested after gold coating in a high vacuum at a voltage of 20 kV.

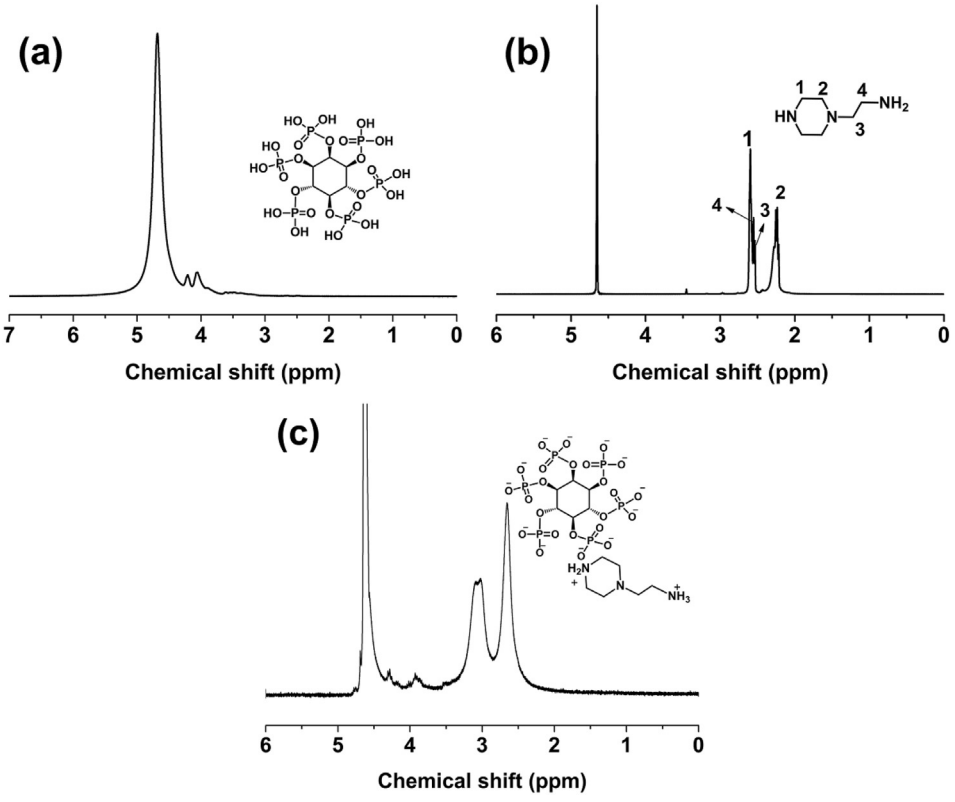

Fig. 2. ^{1}H NMR spectra of PA (a), AEP (b) and PA-AEP (c).

Table 2
Kinetic parameters of the curing reaction with PA-AEP.

		DGEBA/15%PA-AEP	DGEBA/20%PA-AEP
Kissinger[d] and Crane eq[e]	E_a[a]	88.05	108.75
	lnA[b]	15.02	20.33
	n[c]	0.95	0.96
Flynn-Wall-Ozawa eq[f]	E[a]	89.73	110.68

[a] The reaction activation energy in kJ/mol.
[b] Pre-exponential factor in s^{-1}.
[c] Reaction order.
[d] Kissinger equation: $\ln(\beta/T_p^2) = \ln((A \times R)/E_a) - (E_a/R) \times (1/Tp)$.
[e] Crane equation: $\ln\beta = -(E_a/nR) \times (1/T_p) + C$.
[f] Ozawa equation: $\ln\beta + 1.0516 \times (E_a/R) \times (1/T_p) = C'$, β is the heating rate, T_p is the exothermic peak temperature and R is the gas constant.

3. Results and discussion

3.1. Characterization of PA-AEP

Fig. 1 showed IR spectra of N-aminoethylpiperazine (AEP), phytic acid (PA) and ammonium phytic acid (PA-AEP). For AEP, absorption peak at 3274 cm^{-1} and 1120 cm^{-1} belonged to N—H and C—N bonds, respectively [32]. The peaks at 2800-3000 cm^{-1} were assigned to C—H bond. For PA, the peak at 2400 cm^{-1} was assigned to (P=O)—OH. By comparison with AEP and PA, some difference was found in PA-AEP. The peaks at 3274 cm^{-1} (N—H) and 2400 cm^{-1} (-OH) were disappeared. Instead, a new peak appeared at 1528 cm^{-1}, which belonged to NH_3^+ and NH_2^+ bonds [33], suggesting that N—H bonds was changed to NH_3^+ and NH_2^+ bonds after a process of neutralization reaction.

Fig. 2 presented ^1H NMR spectra of raw materials and target product. In Fig. 2, the signal peak at 4.8 ppm belonged to deuterated water. For PA, two peaks at about 4 ppm were observed. For AEP, the peaks at about 2.5–2.6 ppm was ascribed to CH_2- protons of —HN—CH_2-C- and —CH_2-CH_2- group of N—CH_2—CH_2—NH_2, and the

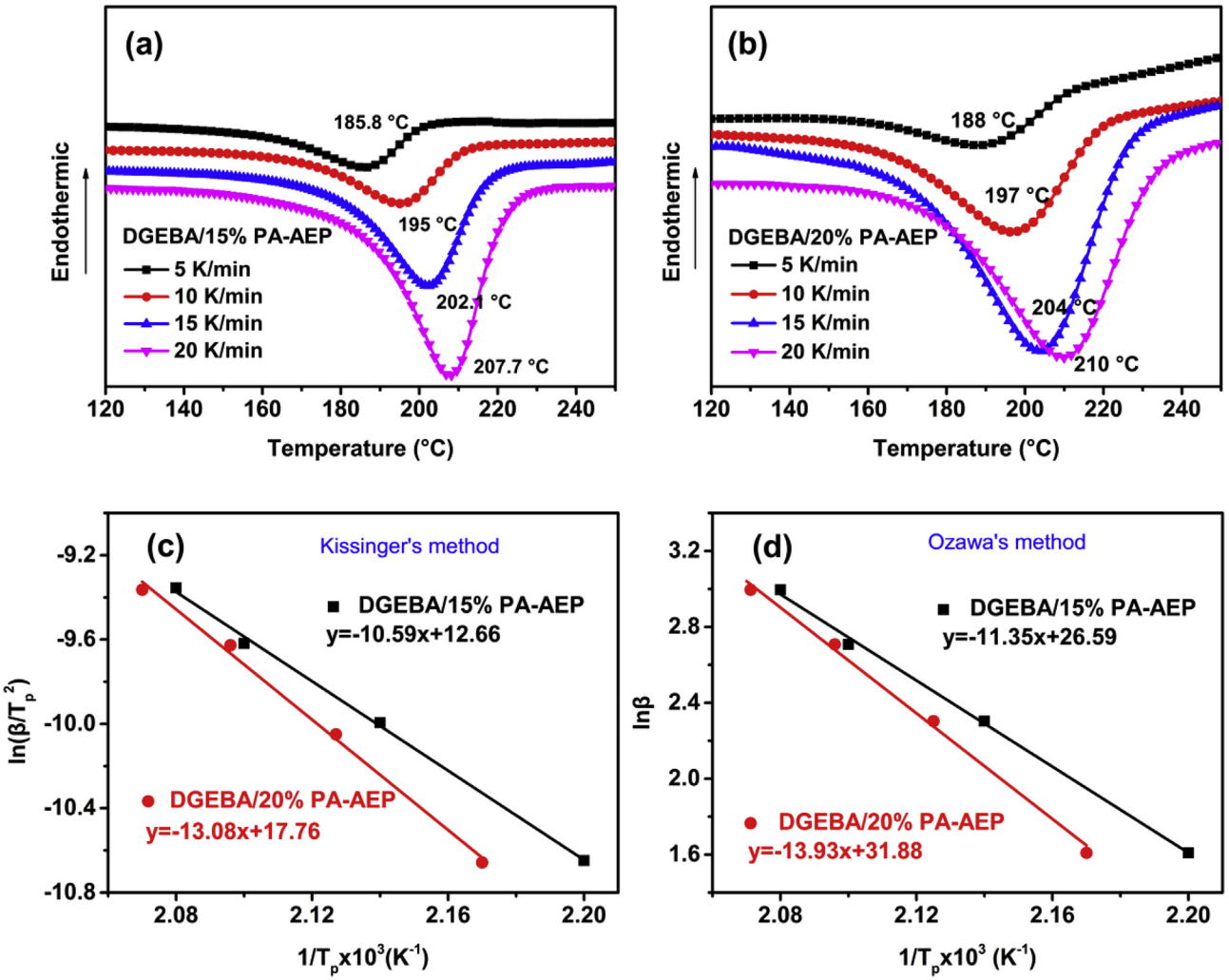

Fig. 4. DSC curves of DGEBA/15% PA-AEP (a) and DGEBA/20% PA-AEP (b) at different heating rates, fitting curves of $\ln(\beta/T_p^2)$ (c) and $\ln\beta$ (d) versus $1/T_p \times 10^3$.

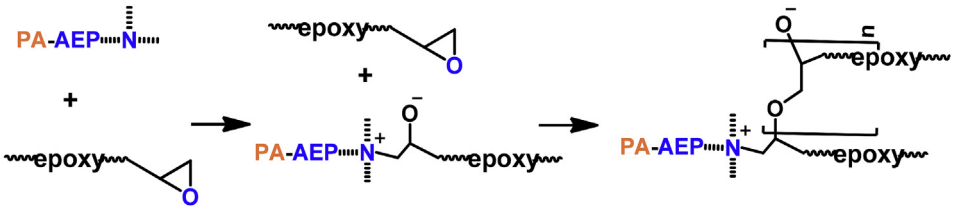

Scheme 1. The curing process of PA-AEP for EP.

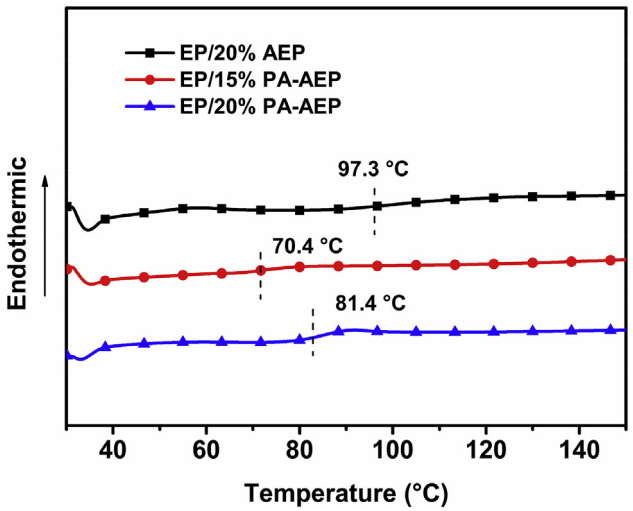

Fig. 5. DSC curves of EP/AEP and EP/PA-AEP samples.

peaks at 2.2–2.4 ppm belonged to $-CH_2$ protons of $-HN-C-CH_2-$. In Fig. 2c, the two peaks at 2.5–2.6 and 2.2–2.4 ppm moved obviously to the left, which indicated the N-aminoethylpiperazine salt with phytic acid was formed.

XPS test was also carried out to further analyze the structure of PA-AEP. As seen in Fig. 3, three peaks appeared in spectra for PA-AEP, which implied that there were three different environments of N atoms in PA-AEP. Herein, the peaks at 400.1, 399.5 and 398.3 eV were assigned to NH_3^+, NH_2^+ and -N- groups [18], respectively. The result of N_{1s} XPS was in agreement with the results of ^1H NMR and FT-IR, suggesting that PA-AEP was prepared successfully.

3.2. Curing

To investigated the influence of PA-AEP on the curing behavior of epoxy resin, the curing kinetics of DGEBA/PA-AEP was studied by nonisothermal DSC testing at different heating rates (5, 10, 15 and 20 K/min). The reaction activation energy (E_a), pre-exponential factor (A) and reaction order (n) were calculated by the Kissinger equation combined with the Crane equation, as shown in Table 2. The Flynn-Wall-Ozawa equation was also applied to verify the E_a values. The three methods are applied to calculate the kinetic parameters without any assumption about a conversion-dependent equation [34]. As shown in Fig. 4, for DGEBA/PA-AEP samples, the

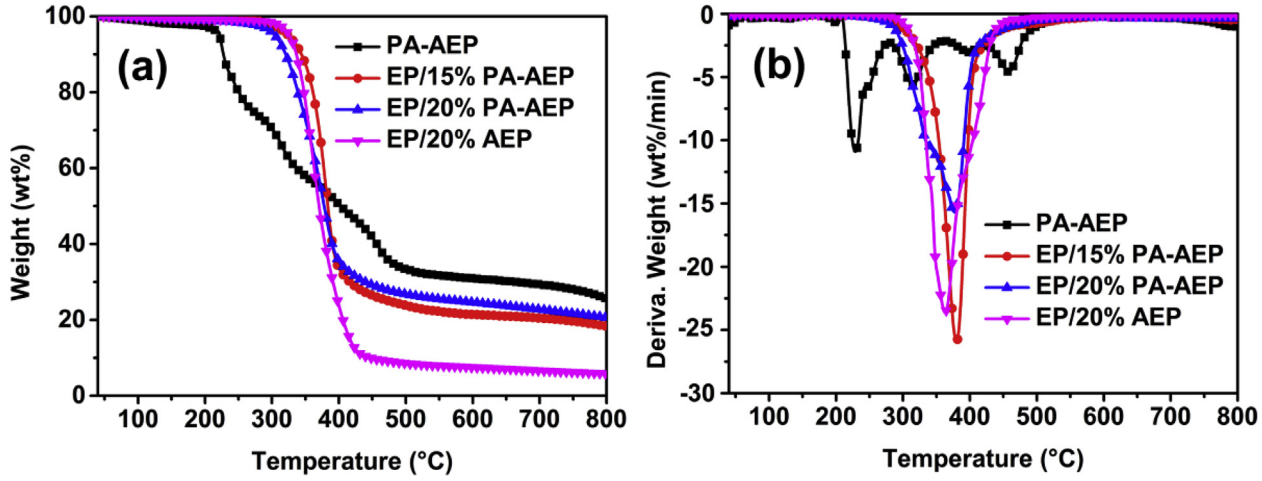

Fig. 6. TGA (a) and DTG (b) curves of PA-AEP, EP/AEP and EP/PA-AEP samples.

Table 3
TGA and DTG data of PA-AEP, EP/AEP and EP/PA-AEP samples.

Sample	$T_{5\%}$ (°C)	T_{max} (°C)	Rate at T_{max} (%/min)	Residue at 800 °C (wt%)
PA-AEP	222.3	227.3/317/459.2	−11.2/-6.1/-4.8	25.6
EP/15% PA-AEP	324.8	382	−26.5	18.4
EP/20% PA-AEP	304.5	375	−17.2	20.6
EP/20% AEP	326.2	364.5	−23.2	5.9

Table 4
Cone calorimeter data of EP/20% AEP and EP/20% PA-AEP.

Sample	EP/20% AEP	EP/20% PA-AEP
TTI (s)	50 ± 1	82 ± 2
t_P (s)	105 ± 3	95 ± 2
PHRR (kW/m^2)	1274 ± 60	708 ± 36
FIGRA ((kW/m^2·s)	12.1	7.5
THR (MJ/m^2)	93.2 ± 2	41.9 ± 1
PSPR (m^2/s)	0.53 ± 0.02	0.27 ± 0.01
TSP (m^2)	68.2 ± 2.5	13.1 ± 0.5
Char residue (wt%)	2.8 ± 0.2	35.2 ± 1

T_p vaules moved toward higher temperature with the increasing of heating rate, which may be due to the fact that the lower heating rate provided longer time for chemical reaction of active groups [35]. Notable, the E_a value of DGEBA/20% PA-AEP was higher than that of DGEBA/15% PA-AEP, which was due to the higher concentration of curing agent PA-AEP which made DGEBA/20% PA-AEP system have more active sites and required higher energy to participate in the chemical reaction at the beginning stage. In addition, The curing reactions of DGEBA/15% PA-AEP as well as DGEBA/20% PA-AEP were both consistent with the n-order kinetic model, where the n values were equal to 0.95 and 0.96, respectively. The above results showed that PA-AEP was an effective curing agent for epoxy.

What's more, according to similar literature reported [18], the curing process for EP/PA-AEP was explained as follows: At a certain temperature, the tertiary nitrogen atom in PA-AEP first reacted with the epoxy groups to form a zwitterion, and then the oxygen anion would further react with another epoxy groups. Here, NH_3^+ and NH_2^+ in PA-AEP which did not react with epoxy groups. The curing route was shown in Scheme 1.

3.3. Thermal analysis

The glass transition temperatures (T_g) of EP/AEP and EP/15% PA-AEP and 20% PA-AEP were investigated by DSC test. As seen in Fig. 5, all samples had a single T_g. In addtion, the T_g vaule of EP/AEP sample were higher than those of EP/PA-AEP, which was ascribled to the higher cross-linking density caused by the higher reactivity of AEP. The T_g vaule of the EP/PA-AEP sample increased with the addition of PA-AEP, which was due to the further increase of the crosslinking density of epoxy with the addition of high concentration of curing agent PA-AEP.

Fig. 6 showed TG and DTG curves of PA-AEP, EP/AEP and EP/PA-AEP samples under N_2 atmosphere, and the relevant data were summarized in Table 3. For PA-AEP, the onset decomposition temperature ($T_{5\%}$, defined as the temperature at which 5 wt% mass loss) was 222.3 °C, and the residues at 800 °C was 25.6%. In Fig. 6a, the thermal decomposition of PA-AEP (as curing agent) showed three degradation stages, in which the temperature at maximum weight loss rate (T_{max}) were 227.3 °C, 317 °C and 459.2 °C,

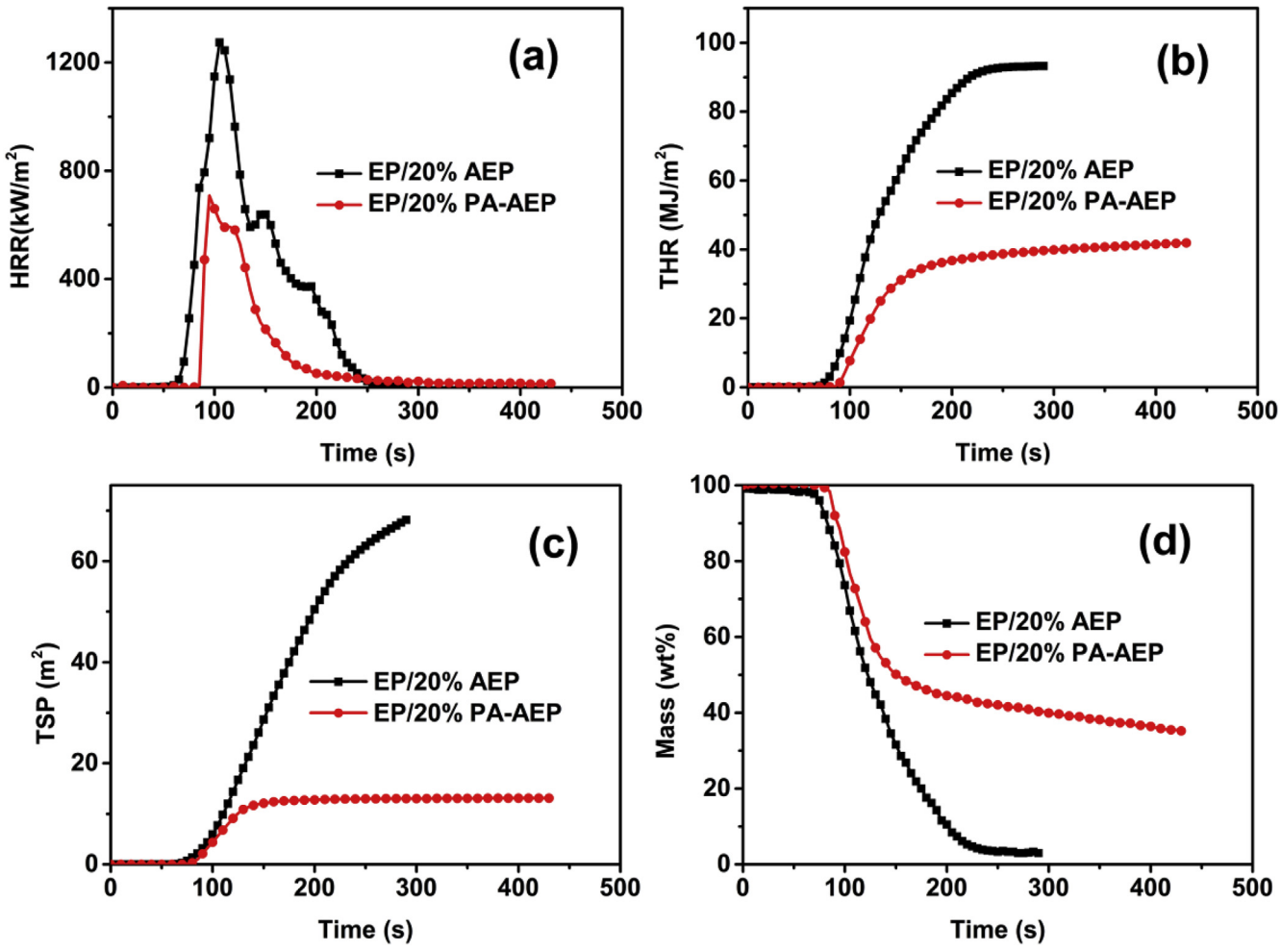

Fig. 7. HRR (a), THR (b), TSP (c) and residual mass (d) curves of EP/20% AEP and EP/20% PA-AEP.

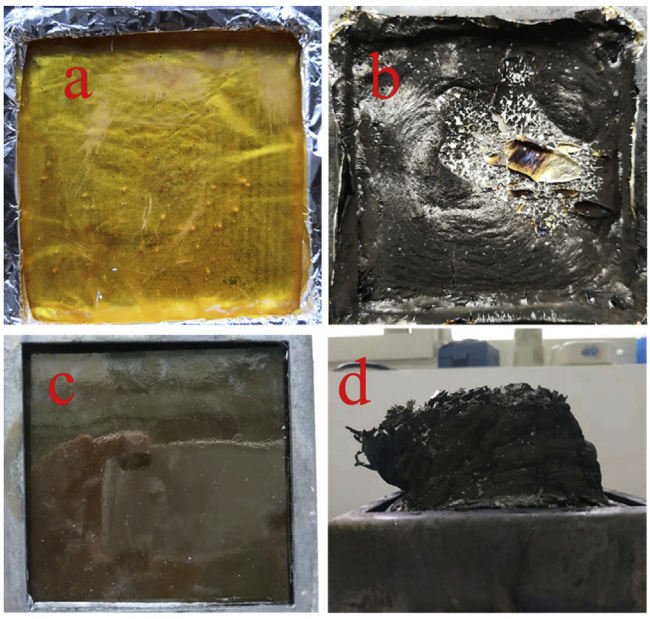

Fig. 8. Digital photos of EP/20% AEP (a, b) and EP/20% PA-AEP (c, d) before and after combustion.

respectively. The first degradation was mainly assigned to the breakage of ionic bonds in PA-AEP and the dehydration reaction of phytic acid [36]. During the second and third steps of decomposition, phosphorus-containing acid and N-aminoethylpiperazine would continue to decompose, and generate NH_3, H_2O, poly-/pyro-/ultraphosphoric acids and other containing the P—N bond compounds, etc [33]. For cured EP samples, due to the addition of PA-AEP, the onset decomposition temperature ($T_{5\%}$) and T_{max} of EP/PA-AEP samples were lower than EP/AEP reference sample, and it decreased continuously with the increase of the PA-AEP. Here, the reasons for the decrease of $T_{5\%}$ and T_{max} were explained as follows: Because the ionic bonds in PA-AEP did not react with epoxy groups, it first gradually broken and decomposed into poly-/pyro-/ultra-phosphoric acids at relative lower temperature, and then the phosphorus-containing acids promoted the dehydration and carbonization of epoxy resin to form a stable carbon. This stable char layer was able to isolate transfer of oxygen and heat. As a result, the residual mass at 800 °C of EP/PA-AEP samples were much higher than EP/AEP reference sample. The higher residual mass implied a positive effect on the flame retardancy.

3.4. Flame retardancy and combustion behavior

Flame retardancy of EP/AEP and EP/PA-AEP samples was first investigated by LOI and UL-94 tests, and relative data were listed in Table 1. As shown in Table 1, the EP/20% AEP reference sample was flammable with only a LOI value of 21.6% and failed to pass UL-94 vertical burning test. By contrast, adding 15 wt% PA-AEP increased the LOI value of EP from 21.6% to 26.5%, but it did not have a positive influence on UL-94 test. As the addition content of PA-AEP increased to 20 wt%, the EP/20% PA-AEP sample passed UL-94 V-0 rating and achieved a LOI value of 28.5%. The above results suggested PA-AEP was an effective flame-retardant curing agent for EP.

Combustion behavior of EP/20% AEP and EP/20% PA-AEP were also investigated by cone calorimeter test and the corresponding data were listed in Table 4. By comparison with EP/20 wt% AEP, the TTI of EP/20% PA-AEP was increased remarkably. This was because the early decomposition of EP/20% PA-AEP produced some non-combustible substances, which would covered the surface of the substrate and slowed down the combustion of the substrate [37]. As seen in Fig. 7, EP/20% AEP reference sample was very flammable and had a sharp the peak of heat release rate (PHRR) value of 1274 kW/m^2, while the PHRR value of EP/20% PA-AEP was decreased to 708 kW/m^2. In addition, unlike EP/20% PA-AEP, the HRR curve of PA-AEP was relatively flat, which indicated that there was an obvious charring process during combustion of EP/20% PA-AEP [38]. As seen in Fig. 8, after cone calorimeter test, EP/20% AEP almost burned out with only 2.8 wt% residual mass, while EP/20%

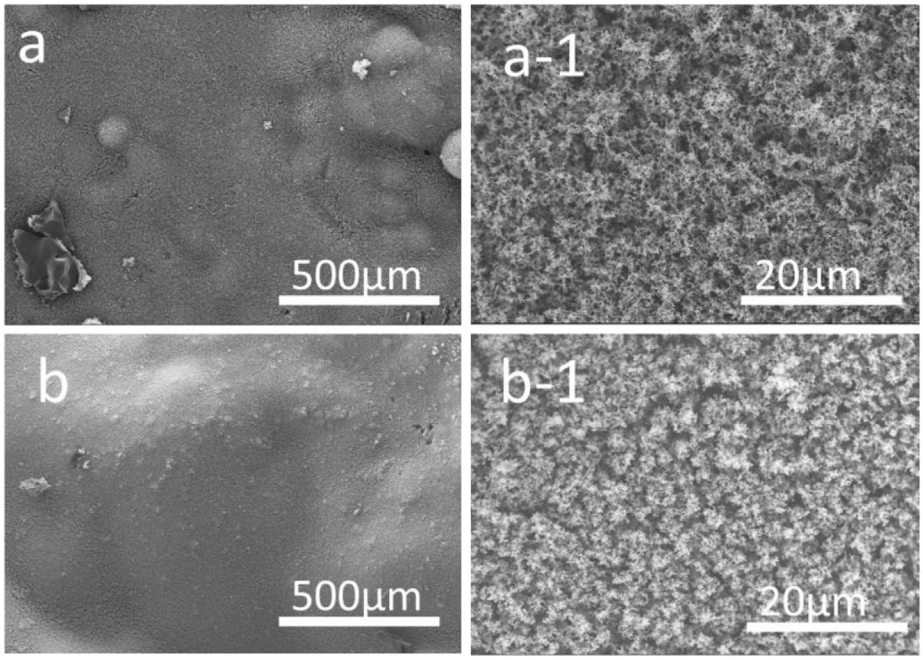

Fig. 9. Morphology of the external char residues for EP/20% AEP (a, a-1) and EP/20% PA-AEP (b, b-1) after cone calorimeter test.

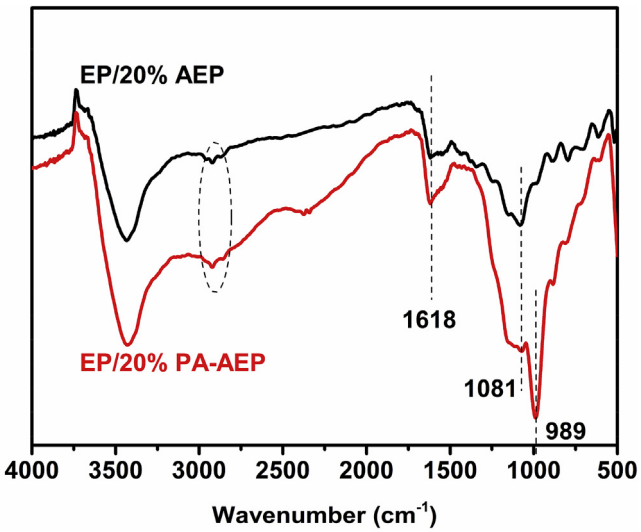

Fig. 10. IR spectra of the chars for EP/20% AEP and EP/20% PA-AEP after cone calorimeter test.

PA-AEP had a large expansive carbon layer (35.2 wt% residual mass), which suggested the existence of condensed phase flame-retardant mechanism. Meanwhile, because of the significant charring effect of EP/20% PA-AEP in the combustion, total smoke product (TSP) and the peak of smoke product rate (PSPR) values were greatly inhibited, and their value were decreased by 80.8% and 49%, respectively. Fire growth rate (FIGRA), defined as the maximum value of HRR/t and was always equal to PHRR/tp, which was used to evaluate the fire safety of materials. As shown in Table 4, the FIGRA value of EP/20% PA-AEP was lower than EP/20% AEP, resulting from the reduction in PHRR. A lower FIGRA value indicated a more escape time in the real life fire scenarios [39].

3.5. Char analysis

The char often has a positive effect on improving the flame retardancy of materials. To better understand the flame-retardant mechanism in condensed phase, the structure and composition of chars after cone calorimeter test was investigated by SEM and IR. Fig. 9 showed SEM images of external chars for EP/20% AEP and EP/20% PA-AEP. In Figs. 9a–1 and b-1, the char layer of EP/20% AEP was a honeycomb structure, while the char layer of EP/20% PA-AEP exhibited relatively compact. Due to the existence of PA-AEP, EP/20% PA-AEP generated phosphorus-containing acids during burning, and then resulting acids catalyzed the cross-linking of EP to form a stable and dense char layer. In addition, the external surface of EP/20% PA-AEP presented bubble-like structure, which was attributed to the release of non-combustible gases. This intumescent and compact char was effective to slow down the transfer of the heat and oxygen, and hence interrupt combustion effectively.

The composition of chars after combustion was analyzed by IR. In Fig. 10, the absorption peaks at about 3000 cm^{-1}, 1618 cm^{-1} and 1081 cm^{-1} were assigned to the stretching vibrations of CH_2-, C=C and C–N bonds, respectively. However, for EP/20% PA-AEP, a new sharp absorption peak appeared at 989 cm^{-1}, which belonged to the stretching vibration of P–O–C bonds, suggesting that there were some organophosphorus and graphite-like complexes exited in chars [40,41]. This result confirmed that phosphorus-containing acids produced by PA-AEP promoted the degradation of EP to form carbon residues rich in P–O–C bond.

3.6. Gaseous products analysis

In order to investigate volatile pyrolysis products of EP/20% AEP and EP/20% PA-AEP during thermal degradation process, TG-IR tests were carried out. Fig. 11 showed FT-IR spectra of gaseous products produced by EP/20% AEP and EP/20% PA-AEP obtained at different temperature ($T_{5\%}$, T_{max}, 400 °C, 450 °C and 500 °C). As seen in Fig. 11, the absorption peaks intensity of gaseous products increased first and then decreased with the increasing of temperature, and reached the maximum at T_{max} (365 and 375 °C), which was consistent with the results of TGA. In addition, the main gaseous products of the degradation of EP/20% AEP and EP/20% PA-AEP were basically the same, including hydrocarbons (2964 cm^{-1}), CO_2 (2350 cm^{-1}), aromatic compounds (1607 and 1510 cm^{-1}) and ether (1260 and 1175 cm^{-1}), which was caused by the decomposition of EP [42]. However, unlike EP/20% AEP, a new peak appeared in IR spectra of EP/20% PA-AEP (from 305 to 500 °C), belonged to NH_3 (965 and 930 cm^{-1}) [43], which was resulted from the decomposition of PA-AEP. Notably, a certain amount of NH_3 released in early stage would dilute the flue gases to slow down burning. At the same time, produced poly-/pyro-/ultraphosphoric

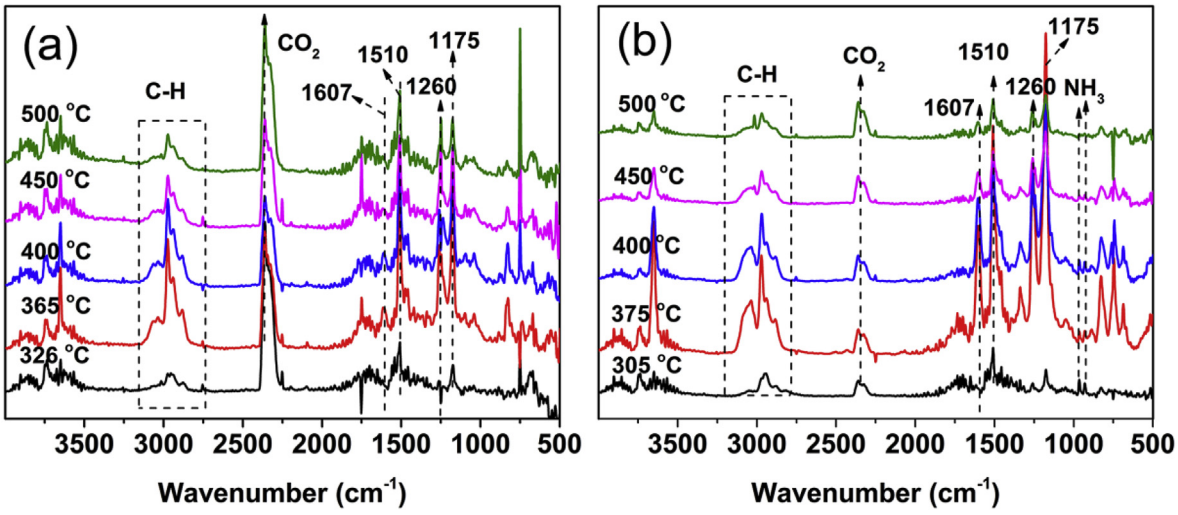

Fig. 11. FT-IR spectra of volatile pyrolysis products of EP/20% AEP and EP/20% PA-AEP after cone calorimeter test.

acids also catalyzed the degradation of EP to form chars. Consequently, an intumescent char would be formed under the blowing effect of NH_3. Furthermore, it was because of the protection of char residues that absorption peaks intensity of gaseous products of EP/20% PA-AEP after 500 °C was lower than that of EP/20% AEP. The above results illustrate that PA-AEP was able to provide both condensed phase shielding effect and the diluting effect in gaseous phase.

4. Conclusions

In this paper, a bio-based macromolecule ammonium phytic acid named PA-AEP was synthesized successfully based on neutralization reaction between phytic acid (PA) and N-aminoethylpiperazine (AEP) and was used as a monocomponent flame-retardant curing agent for improving the flame retardancy and smoke suppression of EP. DSC test result showed PA-AEP effectively cured with epoxy groups. Combustion test results presented the flame retardancy and smoke suppression performance was remarkable enhanced with the addition of PA-AEP. With 20 wt% PA-AEP added, the PA-AEP cured EP sample passed UL-94 V-0 rating and achieved a LOI value of 28%; the THR and TSP values of sample were declined by 55% and 80.8%, respectively. The flame-retardant mechanism was investigated by SEM, IR and TG-IR. The results showed PA-AEP mainly functioned in condensed phase via the formation of a phosphorus-rich intumescent char layer, acted as a barrier to insulate the transfer of heat and oxygen, and hence interrupt combustion.

Acknowledgments

This work was financially supported by the National Natural Science Foundation of China (Grant 51803195).

References

[1] B. Schartel, A.I. Balabanovich, U. Braun, U. Knoll, J. Artner, M. Ciesielski, et al., Pyrolysis of epoxy resins and fire behavior of epoxy resin composites flame retarded with 9, 10-dihydro-9-oxa-10-phosphaphenanthrene-10-oxide additives, J. Appl. Polym. Sci. 104 (2007) 2260–2269.
[2] J. Sun, X. Wang, D. Wu, Novel spirocyclic phosphazene-based epoxy resin for halogen-free fire resistance: synthesis, curing behaviors, and flammability characteristics, ACS Appl. Mater. Interfaces 4 (2012) 4047–4061.
[3] X. Wang, E.N. Kalali, D.Y. Wang, Renewable cardanol-based surfactant modified layered double hydroxide as a flame retardant for epoxy resin, ACS Sustain. Chem. Eng. 3 (2015) 3281–3290.
[4] X. Zhao, H. Babu, J. Llorca, D. Wang, Impact of halogen-free flame retardant with varied phosphorus chemical surrounding on the properties of diglycidyl ether of bisphenol-a type epoxy resin: synthesis, fire behaviour, flame retardant mechanism and mechanical properties, RSC Adv. 6 (2016) 59226–59236.
[5] G. Grause, D. Karakita, J. Ishibashi, T. Kameda, T. Bhaskar, T. Yoshioka, TG-MS investigation of brominated products from the degradation of brominated flame retardants in high-impact polystyrene, Chemosphere 85 (2011) 368–373.
[6] L. Chen, Y.Z. Wang, A review on flame retardant technology in China. Part i: development of flame retardants, Polym. Adv. Technol. 21 (2010) 1–26.
[7] S.D. Jiang, Z.M. Bai, G. Tang, L. Song, A.A. Stec, T.R. Hull, J. Zhan, Y. Hu, Fabrication of Ce-doped MnO_2 decorated graphene sheets for fire safety applications of epoxy composites: flame retardancy, smoke suppression and mechanism, J. Mater. Chem. A. 2 (2014) 17341–17351.
[8] X. Wang, L. Song, H.Y. Yang, W.Y. Xing, B.K. Kandola, Y. Hu, Simultaneous reduction and surface functionalization of graphene oxide with POSS for reducing fire hazards in epoxy composites, J. Mater. Chem. 22 (2012) 22037–22043.
[9] L.P. Gao, D.Y. Wang, Y.Z. Wang, J.S. Wang, B. Yang, A flame-retardant epoxy resin based on a reactive phosphorus-containing monomer of DODPP and its thermal and flame-retardant properties, Polym. Degrad. Stabil. 93 (2008) 1308–1315.
[10] C.S. Wang, H.C. Lin, Synthesis and properties of phosphorus-containing epoxy resins by novel method, J. Polym. Sci., Part A: Polym. Chem. 37 (1999) 3903–3909.
[11] M. El Gouri, A. El Bachiri, S.E. Hegazi, M. Rafik, A. El Harfi, Thermal degradation of a reactive flame retardant based on cyclotriphosphazene and its blend with DGEBA epoxy resin, Polym. Degrad. Stabil. 94 (2009) 2101–2106.
[12] Y. Qiu, L.J. Qian, H.S. Feng, S.L. Jin, J.W. Hao, Toughening effect and flame-retardant behaviors of phosphaphenanthrene/phenylsiloxane bigroup macromolecules in epoxy thermoset, Macromolecules 51 (2018) 9992–10002.
[13] S.Q. Huo, J. Wang, S. Yang, B. Zhang, X. Chen, Q.L. Wu, L.F. Yang, Synthesis of a novel reactive flame retardant containing phosphaphenanthrene and piperidine groups and its application in epoxy resin, Polym. Degrad. Stabil. 146 (2017) 250–259.
[14] Z.B. Shao, M.X. Zhang, Y. Li, Y. Han, L. Ren, C. Deng, A novel multi-functional polymeric curing agent: synthesis, characterization, and its epoxy resin with simultaneous excellent flame retardance and transparency, Chem. Eng. J. 345 (2018) 471482.
[15] S.Q. Huo, J. Wang, S. Yang, C. Li, X.L. Wang, H.P. Cai, Synthesis of a DOPO-containing imidazole curing agent and its application in reactive flame retarded epoxy resin, Polym. Degrad. Stabil. 159 (2019) 79–89.
[16] H.K. Zhang, M.J. Xu, B. Li, Synthesis of a novel phosphorus-containing curing agent and its effects on the flame retardancy, thermal degradation and moisture resistance of epoxy resins, Polym. Adv. Technol. 27 (2016) 860–871.
[17] M.J. Xu, W. Zhao, B. Li, Synthesis of a novel curing agent containing organophosphorus and its application in flame-retarded epoxy resins, J. Appl. Polym. Sci. 131 (2014) 41159–41170.
[18] Y. Tan, Z.B. Shao, X.F. Chen, J.W. Long, L. Chen, Y.Z. Wang, Novel multifunctional organic-inorganic hybrid curing agent with high flame-retardant efficiency for epoxy resin, ACS Appl. Mater. Interfaces 7 (2015) 17919–17928.
[19] B. Liang, J. Cao, X.D. Hong, C.S. Wang, Synthesis and properties of a novel phosphorous-containing flame-retardant hardener for epoxy resin, J. Appl. Polym. Sci. 128 (2013) 2759–2765.
[20] Y.J. Xu, J. Wang, Y. Tan, M. Qi, L. Chen, Y.Z. Wang, A novel and feasible approach for one-pack flame-retardant epoxy resin with long pot life and fast curing, Chem. Eng. J. 337 (2018) 30–39.
[21] B. Schartel, B. Perret, B. Dittrich, M. Ciesielski, J. Kr∈amer, P. Müller, et al., Flame retardancy of polymers: the role of specific reactions in the condensed phase, Macromol. Mater. Eng. 301 (2016) 9–35.
[22] Z.M. Zhu, L.X. Wang, L.P. Dong, Influence of a novel P/N-containing oligomer on flame retardancy and thermal degradation of intumescent flame-retardant epoxy resin, Polym. Degrad. Stabil. 162 (2019) 129–137.
[23] S.B. Deng, W. Liao, J.C. Yang, Z.J. Cao, Y.Z. Wang, Flame-retardant and smoke-suppressed silicone foams with chitosan-based nanocoatings, Ind. Eng. Chem. Res. 55 (2016) 7239–7248.
[24] S. Hu, L. Song, H.F. Pan, Y. Hu, Thermal properties and combustion behaviors of chitosan based flame retardant combining phosphorus and nickel, Ind. Eng. Chem. Res. 51 (2012) 3663–3669.
[25] X.D. Liu, X.Y. Gu, J. Sun, S. Zhang, Preparation and characterization of chitosan derivatives and theirapplication as flame retardants in thermoplastic polyurethane, Carbohydr. Polym. 167 (2017) 356–363.
[26] F. Carosio, J. Alongi, Ultra-fast layer-by-layer approach for depositing flame retardant coatings on flexible PU foams within seconds, ACS Appl. Mater. Interfaces 8 (2016) 6315–6319.
[27] T. Zhang, H.Q. Yan, L. Shen, Z.P. Fang, X.M. Zhang, J.J. Wang, B.Y. Zhang, Chitosan/phytic acid polyelectrolyte complex: a green and renewable intumescent flame retardant system for ethylene-vinyl acetate copolymer, Ind. Eng. Chem. Res. 53 (2014) 19199–19207.
[28] S.L. Qiu, B. Zou, H.B. Sheng, W.W. Guo, J.L. Wang, Y.Y. Zhao, W. Wang, R.K.K. Yuen, Y.C. Kan, Y. Hu, Electrochemically exfoliated functionalized black phosphorene and its polyurethane acrylate nanocomposites: synthesis and applications, ACS Appl. Mater. Interfaces 11 (2019) 13652–13664.
[29] F. Fang, S.Y. Ran, Z.P. Fang, P.G. Song, H. Wang, Improved flame resistance and thermo-mechanical properties of epoxy resin nanocomposites from functionalized graphene oxide via self-assembly in water, Compos. B Eng. 165 (2019) 406–416.
[30] L.Y. Cheng, W.H. Wu, W.H. Meng, S. Xu, H.D. Han, Y.F. Yu, H.Q. Qu, J.Z. Xu, Application of metallic phytates to poly(vinyl chloride) as efficient bio-based phosphorous flame retardants, J. Appl. Polym. Sci. 135 (2018) 46601–46610.
[31] Z. Sang, W.Q. Zhang, Z.Y. Zhou, H.K. Fu, Y.Q. Tan, K.Y. Sui, Y.Z. Xia, Functionalized alginate with liquid-like behaviors and its application in wet-spinning, Carbohydr. Polym. 174 (2017) 933–940.
[32] P.J. Wang, D.J. Liao, X.P. Hu, N. Pan, W.X. Li, D.Y. Wang, Y. Yao, Facile fabrication of biobased P-N-C-containing nano-layered hybrid: preparation, growth mechanism and its efficient fire retardancy in epoxy, Polym. Degrad. Stabil. 159 (2019) 153–162.
[33] Y.Y. Gao, C. Deng, Y.Y. Du, S.C. Huang, Y.Z. Wang, A novel bio-based flame retardant for polypropylene from phytic acid, Polym. Degrad. Stabil. 161 (2019) 298–308.
[34] C. Ma, S.L. Qiu, B. Yu, J.L. Wang, C.M. Wang, W. Zeng, Y. Hu, Economical and environment-friendly synthesis of a novel hyperbranched poly(-aminomethylphosphine oxide-amine) as co-curing agent for simultaneous improvement of fire safety, glass transition temperature and toughness of epoxy resins, Chem. Eng. J. 322 (2017) 618–631.
[35] M. Nonahal, H. Rastin, M.R. Saeb, M.G. Sari, M.H. Moghadam, P. Zarrintaj, B. Ramezanzadeh, Epoxy/PAMAM dendrimer-modified graphene oxide nanocomposite coatings: nonisothermal cure kinetics study, Prog. Org. Coating 114 (2018) 233–243.
[36] Z.M. Zhu, Y.J. Xu, W. Liao, S.M. Xu, Y.Z. Wang, Highly flame retardant expanded polystyrene foams from phosphorus-nitrogen-silicon synergistic adhesives, Ind. Eng. Chem. Res. 56 (2017) 4649–4658.
[37] Z.M. Zhu, W.H. Rao, A.H. Kang, W. Liao, Y.Z. Wang, Highly effective flame

retarded polystyrene by synergistic effects between expandable graphite and aluminum hypophosphite, Polym. Degrad. Stabil. 154 (2018) 1–9.
[38] B. Schartel, T.R. Hull, Development of fire-retarded materials—interpretation of cone calorimeter data, Fire Mater. 31 (2007) 327–354.
[39] R.K. Jian, Y.F. Ai, L. Xia, L.J. Zhao, H.B. Zhao, Single component phosphamide-based intumescent flame retardant with potential reactivity towards low flammability and smoke epoxy resins, J. Hazard Mater. 371 (2019) 529–539.
[40] G. Yang, W.H. Wu, Y.H. Wang, Y.H. Jiao, L.Y. Lu, H.Q. Qu, X.Y. Qin, Synthesis of a novel phosphazene-based flame retardant with active amine groups and its application in reducing the fire hazard of epoxy resin, J. Hazard Mater. 366 (2018) 78–87.
[41] S. Bourbigot, M. Le Bras, R. Delobel, R. Decressain, J.P. Amoureux, Synergistic effect of zeolite in an intumescence process-study of the carbonaceous structures using solid-state NMR, J. Chem. Soc., Faraday Trans. 92 (1996) 149–158.
[42] M.J. Xu, G.R. Xu, Y. Leng, B. Li, Synthesis of a novel flame retardant based on cyclotriphosphazene and DOPO groups and its application in epoxy resins, Polym. Degrad. Stabil. 123 (2016) 105–114.
[43] R.M. Li, C. Deng, C.L. Deng, L.P. Dong, H.W. Di, Y.Z. Wang, An efficient method to improve simultaneously the water resistance, flame retardancy and mechanical properties of POE intumescent flame-retardant systems, RSC Adv. 5 (2015) 16328–16339.